Journal of Alloys and Compounds 713 (2017) 229–235

Contents lists available at ScienceDirect

Journal of Alloys and Compounds

journal homepage: http://www.elsevier.com/locate/jalcom

Morphological, structural and magnetic evolution of sputtered $Fe_{70}Ga_{30}$ thin films upon annealing in oxygen atmosphere

P. Álvarez-Álvarez [a], A. Prados [a], A. Muñoz-Noval [b, c, d], R. Ranchal [a, *]

[a] Dpto. Física de Materiales, Fac. CC. Físicas, Universidad Complutense de Madrid, Madrid 28040, Spain
[b] Department of Applied Chemistry, Hiroshima University, Higashi-hiroshima, Hiroshima 739-8527, Japan
[c] BM25-Spline, The Spanish CRG at the ESRF, Grenoble 38000, France
[d] Instituto de Ciencia de Materiales de Madrid-CSIC, Madrid 28049, Spain

ARTICLE INFO

Article history:
Received 13 June 2016
Received in revised form
24 March 2017
Accepted 14 April 2017
Available online 15 April 2017

Keywords:
Magnetic anisotropy
Fe-Ga alloys
Oxidation

ABSTRACT

We report on the evolution of uncapped $Fe_{70}Ga_{30}$ layers deposited by sputtering and post-growth annealed in oxygen atmosphere in a temperature range from 500 °C to 800 °C. We have investigated the morphology, structure and magnetic properties of films with a thickness of 200 nm deposited on Mo buffer layers on glass substrates. X-ray diffractometry shows a decrease of the lattice parameter up to 600 °C whereas a further increase of the temperature up to 800 °C promotes the transformation to Fe_2O_3. We have observed by x-ray absorption fine structure the partial oxidation of Ga and the formation of Ga aggregates at 600 °C. These aggregates form Ga-rich bubbles that can be observed on the sample surface from which Ga evaporates leaving a Ga-poor layer that is later oxidized into Fe_2O_3. The thermal treatment on oxygen atmosphere has also a clear impact on the magnetic properties of the layers. The uniaxial in-plane magnetic anisotropy of the as-grown film evolves to magnetic isotropy when annealed at 600 °C probably due to the segregation and formation of Ga-rich areas. After Ga evaporates from the sample, Fe is fully oxidized and only a weak ferromagnetism related to Fe_2O_3 is detected.

1. Introduction

In the last years, oxides of Fe-Ga alloys have started to gain attention due to their appealing properties [1–11]. Some of these alloys with a composition around $FeGaO_3$ are piezoelectric with an additional large linear magnetoelectric effect [12]. Other oxides close to the $FeGa_2O_4$ composition have been proposed for hyperthermia treatments and as the insulating paramagnetic layer in a magnetic tunnel junction [13–15]. There are works devoted to the properties of bulk samples [1–3,11,12,16], to thin films and nanoparticles [4–7,9,14–15,17,18]. PLD seems to be one of the most adequate methods to deposit high quality oxide layers in general, and Fe-Ga-O in particular [4–7,17]. Nevertheless, it is a rather expensive and complicated growth technique. An alternative deposition procedure that can be used to achieve oxide thin films is sputtering, although few investigations have reported on the Fe-Ga-O system up-to-date [18].

When using any of the above mentioned growth techniques to obtain Fe-Ga-O oxides, it is of interest the knowledge of the oxidation process of Fe-Ga alloys to better understand and control the growth of the oxides. Although there are papers about the oxidation of Fe and Ga, rather few studies have been published about the oxidation of Fe-Ga films [19]. In the work of *Q. Xing* et al. it is reported the oxidation process in air showing that the formation of surface oxides avoids proper imaging when working in dark-field mode in a transmission electronic microscope. It is mentioned that Ga solution in Fe can prevent macro oxidation process although, to our knowledge, no investigations about this process at high temperatures have been reported. Therefore, we have investigated the morphology, structure, and magnetic properties of sputtered $Fe_{70}Ga_{30}$ thin films when annealed in oxygen atmosphere in a temperature range from 500 °C to 800 °C. In particular, we have studied uncapped layers in order to have a better insight into the process being used a Mo buffer layer in order to avoid oxygen diffusion from the glass substrate into the Fe-Ga. Therefore, the structure of the layers studied in this work is glass/Mo(30 nm)/$Fe_{70}Ga_{30}$(200 nm). Our experimental results show that up to 600 °C, Ga partially oxidized but it also segregates from the Fe matrix forming Ga-rich areas, many of which are observed on the layer surface as round shaped bubbles. A further increase of the

* Corresponding author.
E-mail address: rociran@ucm.es (R. Ranchal).

http://dx.doi.org/10.1016/j.jallcom.2017.04.158
0925-8388/

temperature promotes the Ga evaporation, preferentially from the bubbles, and eventual transformation of the layer into α-Fe_2O_3. Eventually, at 800 °C there are large uncovered areas due to the decomposition of the layer. These results show the difficulties to achieve Ga-Fe-O compounds from the annealing in an oxygen atmosphere of Fe-Ga layers.

2. Experimental techniques

Samples were grown by the DC magnetron sputtering technique at room temperature on glass substrates. The deposition was carried out in oblique incidence with an angle between the vapor beam and the perpendicular to the sample of about 25°. The Fe-Ga films were deposited from a target with a composition of $Fe_{72}Ga_{28}$ using an Ar pressure of 0.3 Pa and a growth power of 70 W in all cases. The distance between substrate and target was of 9 cm that corresponds to the ballistic regime [20]. The Fe-Ga films with a thickness of 200 nm were deposited on top of Mo buffer layers with a thickness of 30 nm also deposited by sputtering in the same previous conditions. These samples were post-annealed in oxygen atmosphere in the temperature range from 500 °C to 800 °C during 1 h.

X-ray diffractometry (XRD) in the Bragg-Brentano configuration was performed in a Philips X'Pert MPD using the Cu K_α wavelength (1.54056 Å). The X-ray absorption fine structure (XAFS) measurements were performed at the Fe K-edge (7112 eV) and the Ga K-edge (10367 eV) in fluorescence yield mode at BM25-Spline at the European Synchrotron (ESRF) in Grenoble (France). For each sample and edge, at least 4 to 5 scans were acquired and merged, in order to increase the signal to noise ratio. The spectra were acquired upon wave-number values of 15 $Å^{-1}$. To obtain the Fourier Transform (FT) of the extended X-ray absorption fine structure (EXAFS) a photoelectron wave-vector (k) range from 2.5 to 12 $Å^{-1}$ was employed for all the spectra. The branch A of the BM25 beamline is equipped with a double Si(111) crystal monochromator of pseudo channel-cut type, refrigerated at 200 K by a Ethanol cooling system. The fluorescence detector is an energy-dispersive 13-elements Si(Li) multidetector from SGX Sensortech. An Fe foil was used to calibrate the energy. EXAFS data were reduced applying standard procedures using the Demeter package [21]. The *ab initio* calculations were performed from crystallographic references of the Ga oxide [22] using CRYSTRALFFREV [23] and FEFF8.4 [24] codes.

The surface composition of the samples and compositional maps were acquired by means of Energy Dispersive X-ray Spectroscopy (EDS) in a JEOL JSM 6400 scanning electron microscope (SEM) operated at 20 kV and 80 mA. Optical images were obtained in an Olympus BX60M microscope. Atomic Force Microscopy (AFM) images were recorded by a Digital Instruments Nanoscope IIIa working in the tapping mode. At room temperature, in-plane hysteresis loops were carried out in a vibrating sample magnetometer (VSM). In the VSM we can rotate the sample being possible to measure the in-plane loops at different angles between the applied magnetic field and the in-plane reference direction, the long side of the substrates [20].

3. Results and discussion

In Fig. 1 we present the XRD diffraction patterns of the as-grown and annealed samples. The as-grown exhibits a main diffraction peak related to the (110) reflection of the α-Fe as generally observed in sputtered Fe-Ga layers [20,25]. The position of this main diffraction peak shifts towards larger angles for annealing temperatures up to 600 °C reflecting a decrease of the lattice parameter in this annealing temperature range (Table 1). This decrease can be due to the formation of Ga-rich areas because of Ga segregation

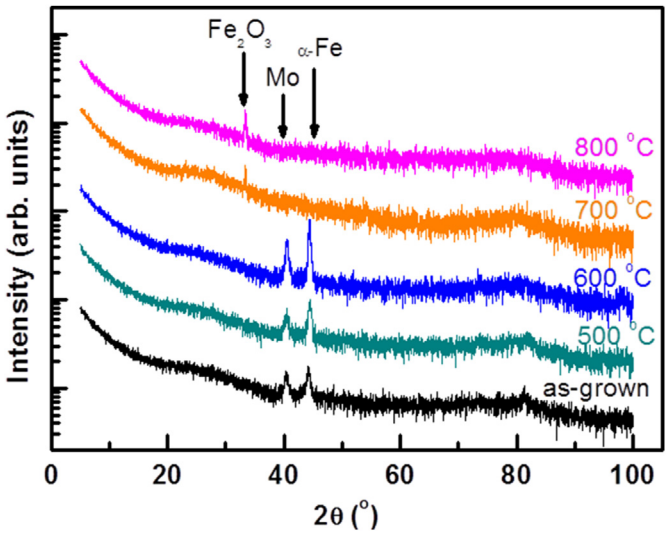

Fig. 1. XRD patterns of the as-grown and annealed samples. The curves have been shifted for clarity.

Table 1
Summary of the lattice parameter (a), intensity of the α-Fe(110) diffraction peak in comparison to that of the Mo buffer, and composition of all the studied samples: Fe and Ga content. In and out refers to the composition measured in and out of a bubble, respectively.

	as-grown	500 °C	600 °C		700 °C	800 °C
a (Å)	2.896	2.881	2.882		–	–
$I_{Fe(110)}/I_{Mo(110)}$	1.1	1.4	1.7		–	–
Fe (at. %)	70	70	In 66	Out 71	94	99
Ga (at. %)	30	30	In 34	Out 29	6	1

that in turn produce an Fe-rich matrix with a lower lattice parameter than the as-grown $Fe_{70}Ga_{30}$ alloy. In addition to this, it is observed an increase of the intensity of the Fe(110) peak that reflects an improvement of the long-range order of the matrix up to 600 °C. This point is also confirmed by the increase of the α-Fe(110) peak intensity ($I_{Fe(110)}$) in comparison to the Mo(110) ($I_{Mo(110)}$) (Table 1). At 700 °C the α-Fe(110) peak disappears and only a reflection that indicates the transformation of the Fe-Ga into Fe_2O_3 can be observed (Fig. 1). The same diffraction pattern remains when annealed at 800 °C. No probes of the formation of any Fe-Ga-O, Fe-Mo or Ga-Mo alloys has been obtained by means of XRD at any temperature.

The selective chemical state of each element in the alloy can be followed along the annealing process by XAFS. We have obtained the XAFS signal of the as-grown and annealed alloys at the Fe and Ga K-edges (Fig. 2). In particular, Fig. 2a shows the XANES, which is sensitive to the chemical state and coordination of the absorbing element, at the Fe K-edge of the as-grown and 600 °C annealed samples compared with the spectrum of metallic bulk Fe. Although the spectrum of the as-grown sample shares several of the main features with the bulk spectrum, such as the shape of the white line and of the edge, it is also similar to the Fe K-edge spectrum obtained in other Ga-rich Fe-Ga alloys [20]. After annealing at 600 °C the resulting spectrum acquires all the features of the metallic Fe in agreement with the XRD data that show an enhancement of the α-Fe diffraction peak. This evolution to a structure more similar to metallic Fe can be taken as an evidence of the migration of Ga from the Fe matrix that is hence losing Ga content.

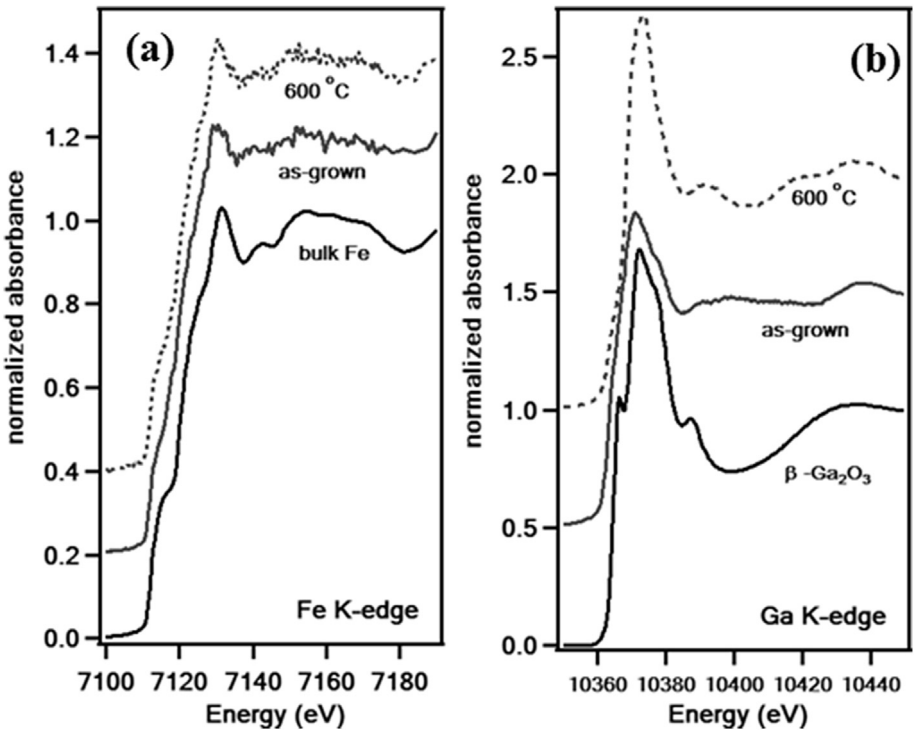

Fig. 2. XANES K-edge spectra for Fe (a) and Ga (b) of the as-grown and annealed at 600 °C Fe-Ga thin films and the references mentioned in the discussion.

The spectra measured at the Ga K-edge give even more information about the annealing process in oxygen atmosphere (Fig. 2b). Again, the spectrum of the as-grown layer resembles that of Ga-rich Fe-Ga films grown in similar conditions that we have already reported [20]. Interestingly, after annealing at 600 °C the shape of the spectrum changes completely. The main peak rises strongly, the resonances after the edge are modified, and the edge shifts to higher energies, an ensemble of effects which may be a sign of increasing the oxidation state. Considering the reported cases in the literature where Ga oxidizes to form β-Ga_2O_3 [19,26], we have performed *ab initio* calculations to obtain the theoretical spectrum of the β-Ga_2O_3 structure in order to qualitatively compare our experimental data. The spectrum of β-Ga_2O_3 also included in Fig. 2b shows that, in average, the features of the Ga XANES spectrum could be qualitatively assigned to the presence of Ga in a mixture of Fe-Ga alloy, Ga oxide and Ga aggregates. In fact, we have performed a rough estimation by fitting the XANES and EXAFS and the phase proportion of Ga in the whole structure may lie on 50/50(20) % of oxide and non-oxide phases pointing out the high content of oxide.

More evidences about the chemical state of Fe and Ga are obtained from the FT of the EXAFS measurements. The FT of the Fe-edge of the as-grown film exhibits characteristics of Fe-Ga alloys that are similar to metallic Fe (Fig. 3a). The first coordination shell is a sum of the first atomic neighbors of Fe, which are on average a mixture of Fe/Ga, depending on the relative composition of the film. The annealing at 600 °C confers to the layer the well-defined structure of the metallic Fe, as it can be observed comparing the relative intensity and position of the main components of the signal. Again, this reflects the crystallinity enhancement of Fe when annealing up to 600 °C.

Respect to the Ga K-edge, the FT shows that after the annealing at 600 °C the component of Ga-O pair is observed in the FT (red arrow in Fig. 3b), but also slight changes in the shape of the FT at longer distances than the first shell. The intensity of the Ga-Ga shell of the metallic phase decreases as a consequence of a combined

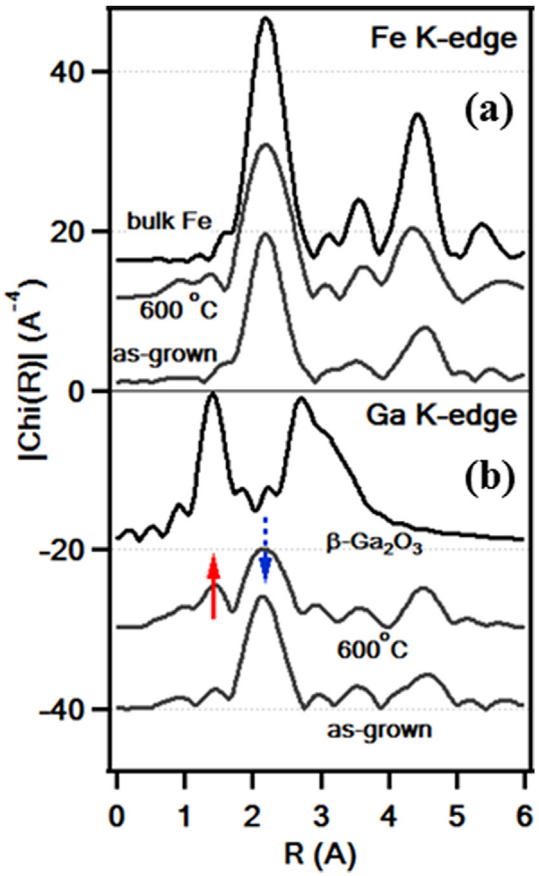

Fig. 3. Fourier transform of the Chi(k) spectra of the Fe (a) and Ga (b) K-edges of the as-grown and annealed at 600 °C Fe-Ga thin films and the references mentioned in the discussion.

effect due to the reduction of the number of atoms at this position, but also because the average distance of this shell reaches a more wide radial distribution, an effect enhanced by the presence of Ga in a mixture of different phases. For comparison, the calculated spectrum of β-Ga_2O_3 has been included to point out the main features. The position of the first shell (Ga-O) matches with the observed component and even the outer shells contribution (a combination of signals which correspond to different Ga-Ga and Ga-O scattering paths) seems to coincide with the observed contribution at ca. 3 Å. Thus, XAFS data show that the oxidation of Fe does not take place when annealing up to 600 °C. However, at this temperature Ga partially oxidize at the same time that form aggregates.

We have observed the film surface by optical microscopy along the annealing process (Fig. 4). Up to 500 °C there are no significant modifications on the Fe-Ga surface respect to the as-grown film

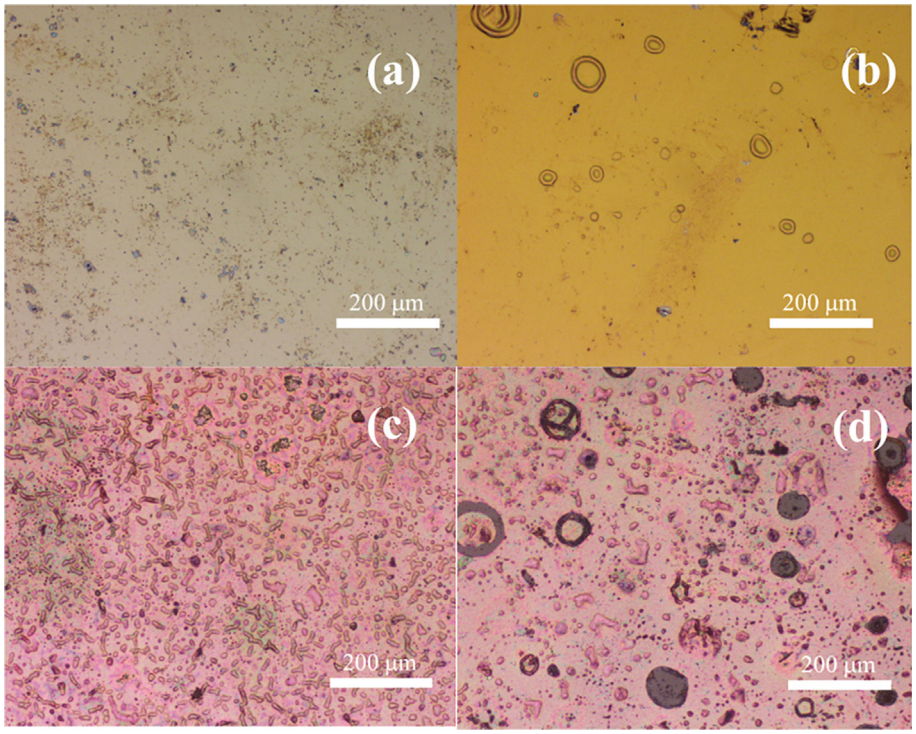

Fig. 4. Optical images of the Fe-Ga surface for different annealing temperatures: (a) 500 °C, (b) 600 °C, (c) 700 °C and (d) 800 °C.

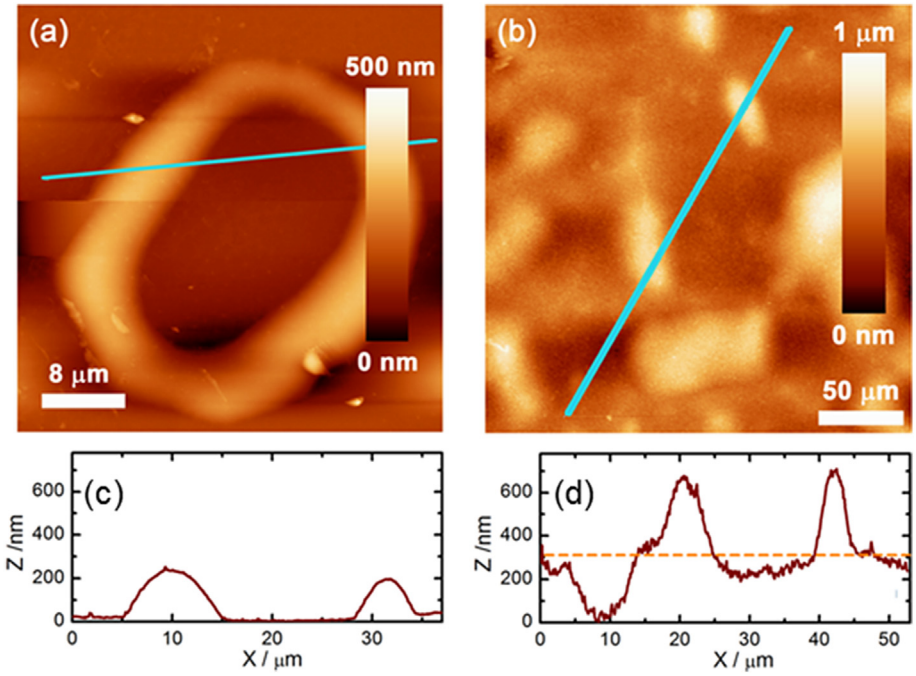

Fig. 5. (a) AFM image of a round-shaped bubble on the surface of a layer annealed at 600 °C. (b) AFM image of elongated bubbles on the surface of a layer annealed at 700 °C. (c) and (d) are the AFM depth profiles measured in the marked lines in (a) and (b), respectively.

(Fig. 4a). At 600 °C, there start to appear round-shaped bubbles with dimensions from 100 μm to only few μm (Fig. 4b). At 700 °C the number of bubbles greatly increases at the same time that their size is reduced. Some uncovered areas are also present on the surface of the layer (Fig. 4c). Eventually, at 800 °C the number of bubbles is much lower but in contrast, the surface shows clear indications of decomposition with big areas of uncovered substrate (Fig. 4d). These results have been further confirmed by AFM (Fig. 5). In the layer annealed at 600 °C we clearly observe the morphology of the round-shaped bubbles being measured a height of around 200 nm for them (Fig. 5a). This suggests their formation upon the accumulation of material during the annealing process up to 600 °C. At 700 °C we observe elongated bubbles with a smaller size that those found at 600 °C in agreement with the optical images (Fig. 5b). In this case, the morphology of the layers shows large height variations evidencing the degradation of the film. The height of the bubbles is 200 nm but we also observe dips with a height close to the Fe-Ga thickness which indicates the first stages of the layer decomposition.

The composition of the Fe-Ga layers as well as compositional maps were acquired in a SEM microscope by EDS (Table 1 and Fig. 6). Also, we have made use of the SEM to image the layer surface. At 500 °C we do not observe any modification of the surface morphology or the Ga content (Table 1) being obtained an homogeneous Fe and Ga distribution in the compositional maps (not shown here). At 600 °C we again confirm the presence of the round-shaped bubbles being possible to measure by EDS the composition in and outside of a bubble. We find a significantly higher Ga content inside the bubbles in comparison to the bubble-free regions (Table 1). At 700 °C, there is a reduction of the Ga content to 6 at. % that indicates the Ga evaporation from the sample (Table 1). The compositional maps for this annealed layer show that the elongated bubbles are in this case poor-Ga regions (Fig. 6a and c, dashed white line). We even detect some uncovered areas, whose morphology remembers that of the elongated bubbles, in which the Fe is even missing (Fig. 6a and b, red line). Eventually, at 800 °C we only detect a residual 1 at. % of Ga indicating the almost complete evaporation of Ga from the layer (Table 1). In this case, the compositional images evidence that the decomposition of the sample has continued and large uncovered regions have been detected (Fig. 6d and e).

Therefore, if we take into account all the experimental results

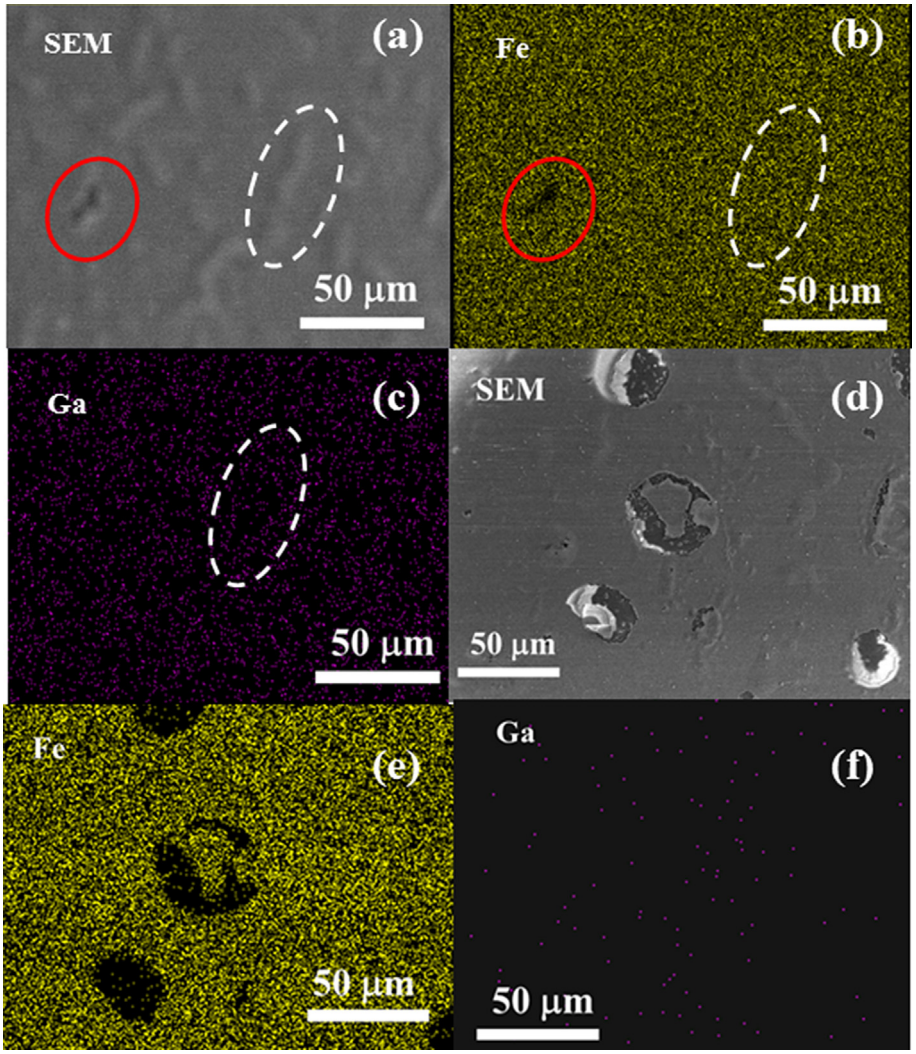

Fig. 6. (a) SEM image of the surface of the sample annealed at 700 °C, (b) and (c) are the compositional maps for Fe and Ga, respectively, of the same area as in (a). In (a), (b) and (c) the white dashed line marks an elongated bubble in which it is observed the absence of Ga but not of Fe. The red solid line in (a) and (b) marks an area in which the sample has started to decompose. (d) SEM image of the sample surface annealed at 800 °C, (e) and (f) are the compositional maps for Fe and Ga, respectively, of the same area as in (d). (For interpretation of the references to colour in this figure legend, the reader is referred to the web version of this article.)

presented so far, we can think on the process as follows. At 500 °C we observe variations on the lattice parameter but not on the morphology or global composition. Then, we can correlate the modification of the lattice parameter with the segregation of Ga to form Ga-rich areas leading to an Fe-enriched more crystallized matrix evidenced by a smaller lattice parameter and improved diffraction patterns. At 600 °C XAFS shows the formation of Ga aggregates that migrate to the surface to form the Ga-rich bubbles as observed by optical images, SEM, and AFM. Also at 600 °C, the Fe-rich matrix continues its crystallization as pointed out by the increase of the diffraction peak intensity whereas part of the Ga starts to be oxidized as revealed by XAFS. This partial oxidation of Ga can be taken place in the Ga-rich bubbles observed at the surface which are areas more exposed to the oxygen atmosphere. The raise of the temperature to 700 °C promotes the evaporation of Ga from the bubbles leaving a Ga-poor matrix. It is beyond this temperature when the Ga-poor matrix oxidizes into α-Fe_2O_3. Therefore, Ga prevents the oxidation of Fe even at high temperatures as we only detect the presence of Fe oxides when Ga has greatly evaporated from the layer. Also, at 700 °C we detect the first stages of the sample decomposition. There are some regions whose morphology resembles that of the elongated bubbles from which Fe has also evaporated. These are the areas at which the decomposition starts. In CoGa intermetallic compounds oxidized at high temperature it is observed the formation of β-Ga_2O_3 due to the Ga diffusion [26]. In a similar way, we have also found evidences of Ga oxides but more interestingly, it is just after the evaporation of Ga from the layer when Fe starts to oxidize. The signals of decomposition are clear at 800 °C. At this temperature, the uncovered regions have greatly increased in number and size.

Considering the evolution of the morphology and structure of $Fe_{70}Ga_{30}$ thin films during annealing in oxygen atmosphere, it is also of great interest to study the evolution of the magnetic properties. The as-grown layer has an in-plane uniaxial magnetic anisotropy (Fig. 7a) as already reported in Fe-Ga films deposited under the same growth conditions, ballistic regime and 70 W of growth power, and similar Ga content [20]. The layer annealed at 500 °C still exhibits this magnetic anisotropy with an increased coercivity which can be related to the loss of Ga and partial crystallization of the Fe matrix as indicated by XRD. The effect of the thermal treatment on the modification of the magnetic behavior continues at 600 °C when the magnetic anisotropy disappears and the layer shows an isotropic in-plane magnetic behavior with a larger coercivity (Fig. 7b). Although it might be expected an increase of the anisotropy because of the crystallization of the Fe-rich matrix, the experimental results indicate a completely different magnetic behavior. Sputtered Fe-Ga layers in the diffusive flow regime also show in-plane magnetic isotropy [20]. In that case, it was correlated to the presence of a high fraction of the A2 disordered phase, of Ga-rich nanoaggregates and the inhomogeneities promoted by these phases. Here, we have found large Ga-rich regions (even Ga-rich bubbles on the layer surface) and a high crystallization of the Fe-rich matrix. This crystallization seems not to enhance the magnetic anisotropy and therefore, structural degradation caused by the partial Ga oxidation, Ga segregation and formation of Ga-rich regions and the inhomogeneities associated to all these effects are proposed as a cause of the observed magnetic isotropy. The increase of the annealing temperature up to 700 °C promotes the reduction of the ferromagnetic contribution (Fig. 7c). Although we can observe some hysteresis in the magnetization curve, the diamagnetic signal related to the substrate is the main contribution. We can understand this result taking into account that at 700 °C the Fe-Ga has transformed into α-Fe_2O_3 (hematite) which is a well know antiferromagnetic material. At 800 °C, the ferromagnetic signal is almost vanished due to the sample decomposition.

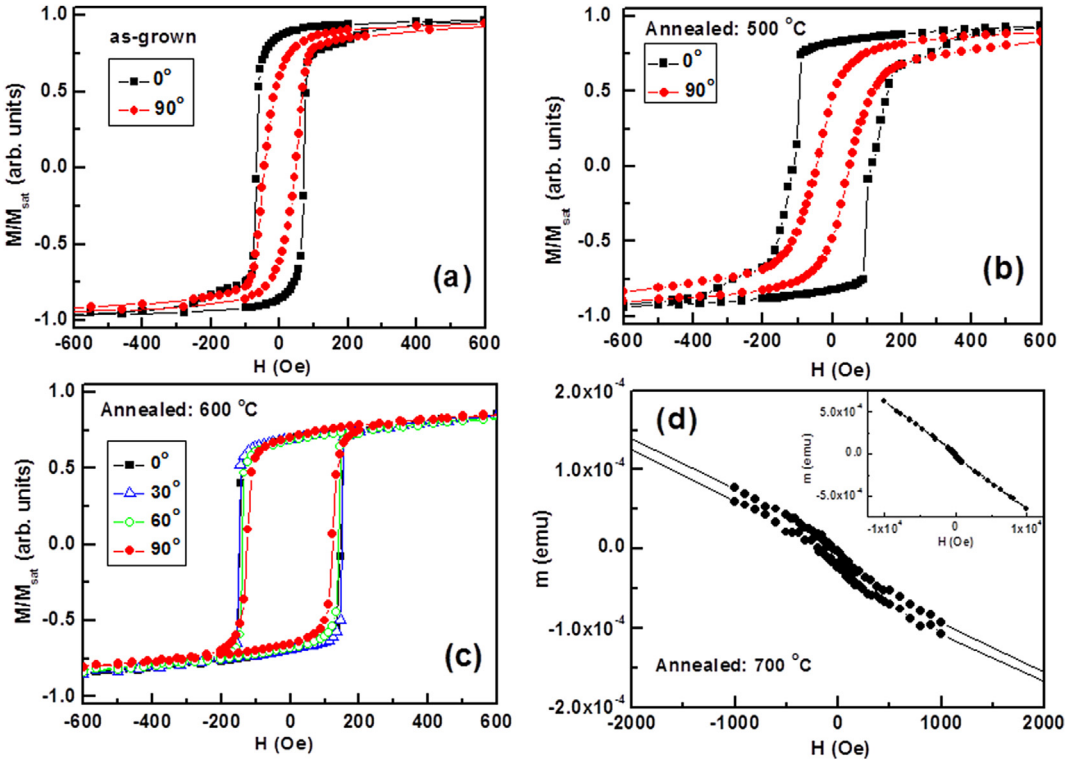

Fig. 7. Hysteresis loops measured at room temperature at different angles between the reference direction and the in-plane magnetic field: (■) 0°, and (●) 90° (a) as-grown layer and (b) annealed at 500 °C. (c) Hysteresis loops measured at room temperature of a Mo/$Fe_{70}Ga_{30}$ layer annealed at 600 °C at different angles between a reference direction and the in-plane magnetic field: (■) 0°, (Δ) 30°, (○) 60°, and (●) 90°. (c) Hysteresis loop measured at room temperature of a Mo/$Fe_{70}Ga_{30}$ layer annealed at 700 °C.

4. Conclusions

In summary, we have monitored the evolution of sputtered $Fe_{70}Ga_{30}$ thin films during annealing in oxygen atmosphere in a temperature range from 500 °C to 800 °C. The annealing promotes Ga segregation and the formation of Ga-rich aggregates which we have clearly observed at 600 °C by XAFS. Whereas at this temperature we obtain indications of the Ga oxidation, Fe still is in its metallic state. The Ga aggregates form round-shaped bubbles at the layer surface from which Ga evaporates at 700 °C. It is at this temperature when the Ga-poor layer oxidizes into α-Fe_2O_3. Further increase of the temperature upon 800 °C only produces the decomposition of the layer. The thermal treatment in oxygen atmosphere has a clear impact on the magnetic properties of the layers. At 600 °C, the in-plane magnetic anisotropy disappears probably as a consequence of the formation of Ga-rich precipitates and inhomogeneities present in the layer. Further increase of the temperature fully oxidizes the Fe to antiferromagnetic α- Fe_2O_3 phase. Our results show that the annealing in an oxygen atmosphere of an $Fe_{70}Ga_{30}$ layer is not an adequate route to produce Fe-Ga-O oxides.

Acknowledgments

This work has been financially supported through the projects MAT2015-66888-C3-3-R of the Spanish Ministry of Economy and Competitiveness (MINECO/FEDER) and PR26/16-3B-2 of Santander and Universidad Complutense de Madrid. We thank “CAI Difracción de rayos-X” of UCM for the X-ray diffractometry measurements, “Centro Nacional de Microscopía” of UCM for EDS measuresuments and Instituto of Sistemas Optoelectrónicos y Microtecnología (ISOM) for using its facilities for the growth and magnetic characterization of the samples. We also want to thank BM25-Spline, the Spanish CRG at ESRF for providing beamtime.

References

[1] T. Arima, D. Higashiyama, Y. Kaneko, J.P. He, T. Goto, S. Miyasaka, T. Kimura, K. Oikawa, T. Kamiyama, R. Kuumai, Y. Tokura, Phys. Rev. B 70 (2004) 064426.
[2] M. Bakr Mohamed, A. Senyshyn, H. Ehrenberg, H. Fuess, J. Alloys Compd. 492 (2010) L20.
[3] W. Kim, J.H. We, S.J. Kim, C.S. Kim, J. Appl. Phys. 101 (2007) 09M515.
[4] K. Sharma, V. Raghavendra Reddy, A. Gupta, R.J. Choudhary, D.M. Phase, V. Ganesan, Appl. Phys. Lett. 102 (2013) 212401.
[5] M. Trassin, N. Viart, G. Versini, S. Barre, G. Pourroy, J. Lee, W. Jo, K. Dumesnil, C. Dufour, S. Robert, J. Mater. Chem. 46 (2009) 8876. PLD.
[6] S.H. Oh, J.H. Lee, R.H. Shin, Y. Shin, C. Meny, W. Jo, Appl. Phys. Lett. 106 (2015) 142902.
[7] A. Roy, S. Mukherjee, S. Sarkar, S. Auluck, R. Prasad, R. Gupta, A. Garg, J. Phys. Condens. Matter 24 (2012) 435501.
[8] S.G. Bahoosh, J.M. Wesselinowa, J. Appl. Phys. 113 (2013) 063905.
[9] K. Kaneko, I. Kakeya, S. Komori, S. Fujita, J. Appl. Phys. 113 (2013) 233901.
[10] J. Atanelov, P. Mohn, Phys. Rev. B 92 (2015) 104408.
[11] V.R. Reddy, K. Sharma, A. Gupta, A. Banerjee, J. Magn. Magn. Mater. 362 (2014) 97.
[12] G.T. Rado, Phys. Rev. Lett. 13 (1964) 335.
[13] C.C. Huang, C.H. Su, M.-Y. Liao, C.-S. Yeh, Phys. Chem. Chem. Phys. 11 (2009) 6331–6334.
[14] J. Sánchez, D.A. Cortés-Hernández, J.C. Escobedo-Bocardo, R.A. Jasso-Terán, A. Zugasti-Cruz, J. Mater. Sci. Mater. Med. 25 (2014) 2237.
[15] L.M.B. Alldredge, R.V. Chopdekar, B.B. Nelson-Cheeseman, Y. Suzuki, Appl. Phys. Lett. 89 (2006) 182504.
[16] J.P. Remeika, J. Appl. Phys. 31 (1960) S263.
[17] S. Mukherjee, A. Roy, S. Auluck, R. Prasad, R. Gupta, Ashish Garg, Phys. Rev. Lett. 111 (2013) 087601.
[18] J.M.D. Coey, E. Devlin, R.J. Gambino, J. Appl. Phys. 53 (1982) 7810.
[19] Q. Xing, M.J. Kramer, D. Wu, T.A. Lograsso, Mater. Charact. 61 (2010) 598.
[20] A. Muñoz-Noval, A. Ordóñez-Fontes, R. Ranchal, Phys. Rev. B 93 (2016) 214408.
[21] B. Ravel, M. Newville, J. Synchrotron Radiat. 12 (2005) 537.
[22] G. Ahman, J. Svensson, J.A. Albertsson, Acta Crystallogr. Sect. C 6 (1996) 1336.
[23] A. Michalowicz, J. Moscovici, D. Bouvet-Muller, K. Provost, J. Phys. 190 (2009) 12034.
[24] A.L. Ankudinov, B. Ravel, J.J. Rehr, S.D. Conradson, Phys. Rev. B 58 (1998) 7565.
[25] R.A. Dunlap, N.C. Deschamps, R.E. Mar, S.P. Farrell, J. Phys. Condens. Matter 18 (2006) 4907.
[26] U. Koops, D. Hesse, M. Martin, J. Mater. Res. 17 (2002) 2489.